

# APPLICATION OF INDEPENDENT COMPONENT ANALYSIS FOR BEAM DIAGNOSIS \*

X. Huang<sup>†</sup>, S. Y. Lee, Indiana University, Bloomington, IN 47405, USA  
Eric Prebys, Ray Tomlin, Fermilab, Batavia, IL 60510, USA

## Abstract

The independent component analysis (ICA) is applied to analyze simultaneous multiple turn-by-turn beam position monitor (BPM) data of synchrotrons. The sampled data are decomposed to physically independent source signals, such as betatron motion, synchrotron motion and other perturbation sources. The decomposition is based on simultaneous diagonalization of several unequal time covariance matrices, unlike the model independent analysis (MIA), which uses equal-time covariance matrix only. Consequently the new method has advantage over MIA in isolating the independent modes and is more robust under the influence of contaminating signals of bad BPMs. The spatial pattern and temporal pattern of each resulting component (mode) can be used to identify and analyze the associated physical cause. Beam optics can be studied on the basis of the betatron modes. The method has been successfully applied to the Booster Synchrotron at Fermilab.

## INTRODUCTION

The transverse motion of a beam in a synchrotron is composed of components driven by various physical factors. These components include the betatron motion, synchrotron motion and possibly other sources. A synchrotron often has many BPMs around the ring to detect the beam transverse orbit and in many synchrotrons the BPMs are capable of measuring the orbit on turn-by-turn basis. The multiple simultaneous turn-by-turn orbit measurements provide vast data which allow us to study the physical factors that affect the beam. It is highly desirable to separate the contributions of the factors and study them individually. The model independent analysis (MIA) [1] is a first attempt to achieve the goal. MIA is a principal component analysis (PCA). It can be used to study coherent betatron oscillations without a lattice model and is able to reduce random noises. It has been applied to some electron storage rings successfully and is now an established efficient beam diagnostic tool.

However, due to its PCA nature, MIA does not accomplish complete mode isolation. The linear coupling of betatron motions can still be mixed. The synchrotron motions, if not filter out, can also be mixed with betatron motions. The other less-significant sources are more likely to mix because their variances are close in strength.

In this paper we introduce the application of independent component analysis (ICA) for multiple turn-by-turn BPM data analysis to overcome the difficulties of MIA.

The ICA method considers turn-by-turn BPM data as linear mixtures of independent source signals. We further assume the source signals are narrowband signals. Hence their spectra must not overlap because of the independence and the un-equal time covariance matrices must be diagonal. The source signals and the mixing matrix can be found by jointly diagonalizing the un-equal time covariance matrices of the sample data with a few time-lag constants. The spatial and temporal properties of the resulting modes can be used to identify the origins of the source signals.

This method can successfully separate the linear coupling normal modes, the synchrotron modes and other modes. It is more robust than MIA because of the use of more statistical information of the source signals. It is less sensitive to influences of bad BPMs.

Applying this new method to Fermilab Booster data, we have measured the linear lattice functions and extracted synchrotron oscillations.

## THE ICA FOR BEAM DIAGNOSIS

Suppose there are  $m$  BPMs around the ring and each records the orbit for  $N$  turns. We put the readings of all BPMs into an  $m \times N$  data matrix  $\mathbf{x}$  such that each row represents the readings of one BPM. The offset of each row is subtracted from the raw readings. The data matrix is related with the source matrix  $\mathbf{s}$  by

$$\mathbf{x}_{m \times N} = \mathbf{A}_{m \times n} \mathbf{s}_{n \times N} + \mathcal{N}_{m \times N} \quad (1)$$

where  $n$  (not known a priori) is the number of source signals,  $\mathbf{A}$  is the mixing matrix,  $\mathcal{N}$  contains random noises. The un-equal time covariance matrix of source signals defined by  $\mathbf{C}_s(\tau) \equiv \langle \mathbf{s}(t)\mathbf{s}(t+\tau)^T \rangle$  is diagonal because the source signals are non-overlapping narrowband signals. The time-lag constant  $\tau$  must be an integer. It follows from Eq. (1) that  $\mathbf{C}_x(0) = \mathbf{A}\mathbf{C}_s(0)\mathbf{A}^T + \sigma^2\mathbf{I}$  and  $\mathbf{C}_x(\tau) = \mathbf{A}\mathbf{C}_s(\tau)\mathbf{A}^T, \tau \neq 0$ , i.e., the mixing matrix  $\mathbf{A}$  is the diagonalizer of the sample covariance matrix  $\mathbf{C}_x$ , where we have assumed the noises are white and independent of the source signals and  $\sigma$  denotes the noise level.

The source signals and the mixing matrix can be found with the Second-Order Blind Identification (SOBI) algorithm [2]. First, we perform eigen-decomposition of the sample covariance matrix  $\mathbf{C}_x(0)$  and collect the  $n$  largest eigenvalues into a diagonal matrix  $\mathbf{\Lambda}_1$  and the associated eigenvectors into matrix  $\mathbf{U}_1$ . The number  $n$  is chosen such that the eigenvalues representing noise background are excluded. An intermediate "whitened" data matrix is constructed with  $\xi = \mathbf{V}\mathbf{x}$ , where  $\mathbf{V} \equiv \mathbf{\Lambda}_1^{-1/2}\mathbf{U}_1^T$ . This step is equivalent to MIA while  $\xi$  contains its temporal vectors and  $\mathbf{U}_1$  contains the spatial vectors.

\* Work supported by grants from DE-AC02-76CH03000, DOE DE-FG02-92ER40747 and NSF PHY-0244793

<sup>†</sup> xiahuang@fnal.gov

Second, we compute the time-lagged covariance matrices of  $\xi$  by  $\{C_\xi(\tau_k) = \langle \xi(t)\xi(t + \tau_k)^T \rangle\}$  for a selected set of time-lag constants  $\tau_k$ . We form symmetric matrices  $\overline{C}_\xi(\tau_k) = (C_\xi(\tau_k) + C_\xi(\tau_k)^T)/2$  and find an orthonormal matrix  $\mathbf{W}$  that diagonalizes all matrices  $\overline{C}_\xi(\tau_k)$  of this set, i.e.  $\overline{C}_\xi(\tau_k) = \mathbf{W}\mathbf{D}_k\mathbf{W}^T$ , where  $\mathbf{D}_k$  is diagonal. In practice, joint diagonalization can be achieved only approximately. Algorithms for approximate joint diagonalization can be found in Ref. [3].

Finally, the source signals and the mixing matrix are  $\mathbf{s} = \mathbf{W}^T\mathbf{V}\mathbf{x}$  and  $\mathbf{A} = \mathbf{V}^{-1}\mathbf{W}$  respectively, where  $\mathbf{V}^{-1} = \mathbf{U}_1\mathbf{\Lambda}_1^{1/2}$ . A row vector of  $\mathbf{s}$  and the corresponding column of  $\mathbf{A}$  is called the temporal and spatial vector of a mode, respectively. The properties of the temporal and spatial vectors can help the identification of their physical origins. For example, the betatron modes always come in pairs because each BPM sees different phases and its temporal vectors are oscillations with proper tunes and decoherence. The spatial vectors of the betatron modes can be used to calculate beta functions and phase advances. The spatial vector of the synchrotron mode is proportional to the dispersion function and the temporal vector has synchrotron tune.

The betatron function and phase advance can be derived from the spatial vectors of the paired betatron modes

$$\beta_i = a^2(A_{b1,i}^2 + A_{b2,i}^2), \quad \psi_i = \tan^{-1} \left( \frac{A_{b1,i}}{A_{b2,i}} \right) \quad (2)$$

where  $a$  is a constant depending on initial conditions. Then dispersion  $D_x$  and momentum deviation  $\delta(t)$  are related to the spatial vector and temporal vector of the synchrotron mode by

$$\mathbf{D} = b\mathbf{A}_s, \quad \delta(t) = s_s(t)/b \quad (3)$$

with a constant  $b$ . The constant  $a$ ,  $b$  could be ‘‘determined’’ by certain calibration procedure with other measurements. In our study, we often just scale the spatial vectors up to compare with the beta function and dispersion of model calculation.

We have tested the applicability of both the ICA method and MIA with simulations [4]. The results show that MIA modes get mixed when the source signals have close variances and ICA is free of such mixing. Because of its better capability of mode separation, ICA is more robust under the effect of bad BPMs. The dependence of the separation on finite sampling is also studied.

The ICA for beam diagnosis has found applications at Fermilab Booster and APS. Fig. 1 shows examples of the temporal vectors for APS data. The beam was excited by a sudden shift of synchronous phase. The spatial vectors were used to compute the beta function and dispersion [5].

## APPLICATION TO FERMILAB BOOSTER

Fermilab Booster has 48 BPMs, all of them are able to measure turn-by-turn orbit for both transverse planes. We have taken turn-by-turn data in two setup modes of the

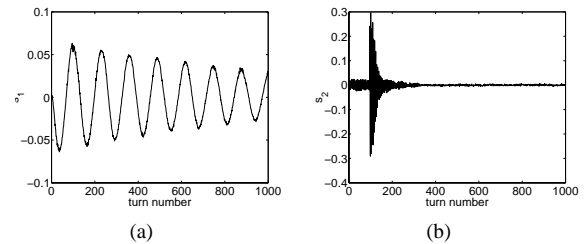


Figure 1: The temporal vectors of (a) the synchrotron mode, (b) one of the betatron modes, of an APS data set. Data taken by Weiming Guo at APS.

Booster. In the DC mode the beam was kept in injection energy (400 MeV) for the whole cycle (1/30 s) and in the AC mode beam energy was ramped from 400 MeV to 8 GeV as in normal operations. The beam was excited by a horizontal pinger which is fired every 0.5 ms with a pulse width of 2.2  $\mu$ s, or one turn at injection. Each cycle has 15200 turns (DC) or 20000 turns (AC). We often divide the cycles into small pieces so that each piece starts with the firing of the pinger and ends before the next firing, about 220 turns per piece. Since we have both the horizontal and vertical BPM data, we put them into one data matrix  $\mathbf{y} = \begin{pmatrix} \mathbf{x} \\ \mathbf{z} \end{pmatrix}$  for ICA analysis. Such arrangements help the mode separation, especially for the modes appearing in both horizontal and vertical BPMs, e.g., the linearly coupled betatron motions. The data presented in this paper were taken after the 2003 shutdown when one of the two extraction doglegs was re-positioned to alleviate the dogleg effects.

For data taken in DC mode, we have measured the beta functions, phase advances and dispersion function. Fig. 2 shows the temporal and spatial vectors of a pair of horizontal betatron modes as an example. The spatial vectors are used to calculate the beta function and phase advances with Eq. (2). The results are compared to the existing lattice model in Fig. 3. The error bars are estimated with 20 pieces of data from two data sets. The average error bars are 6% for  $\sigma_\beta/\beta$  and 0.03 rad for  $\sigma_\psi$ .

The temporal vector and the spatial vector of the dispersion mode are used to calculate  $\frac{\Delta p}{p}$  and dispersion function  $D_x$  as shown in Fig. 4. This mode is from a data piece of 1000 turns right after injection. The injection energy mismatch is  $\frac{\Delta p}{p} = -0.4 \times 10^{-3}$  initially and is damped by the longitudinal damper in about 300 turns. The error bars in Fig. 4(b) are estimated with multiple data sets, which gives  $\sigma_D/D = 4\%$ . The measurements of the linear lattice functions indicate that our existing lattice model approximate the real Booster to a reasonable level yet still with considerable discrepancies.

We have also observed instability modes in DC data sets. Fig. 5 shows an example in the region from turn 4001 to turn 6000. Noticeably the amplitude plots Fig. 5(a) indicates this instability mode appears only in half of the ring where the RF cavities sit. However, the cause of the insta-

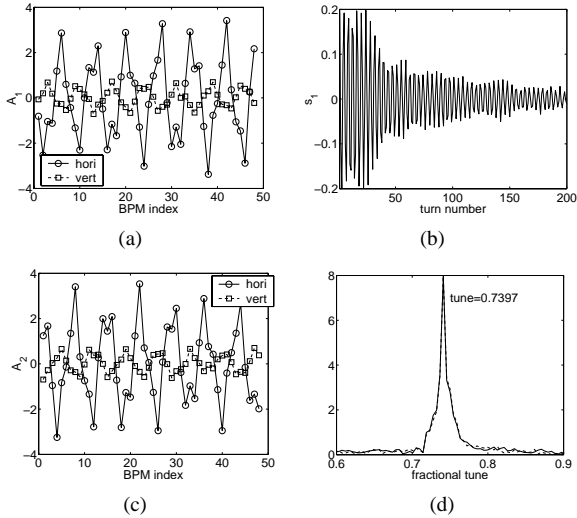


Figure 2: The betatron modes of Booster DC data. (a), (c) spatial vectors of betatron mode 1, 2. (b) temporal vector of mode 1. (d) FFT spectra of the temporal vectors.

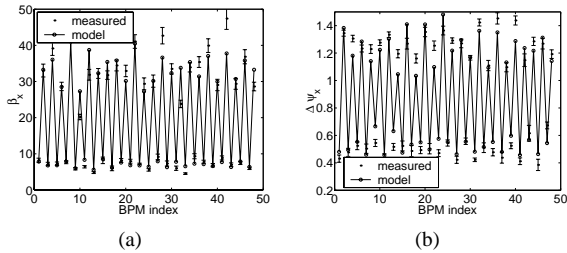


Figure 3: The measured horizontal beta function (a) and phase advance (b) are compared to model calculations. The phase advances in (b) is measured from one BPM to the next.

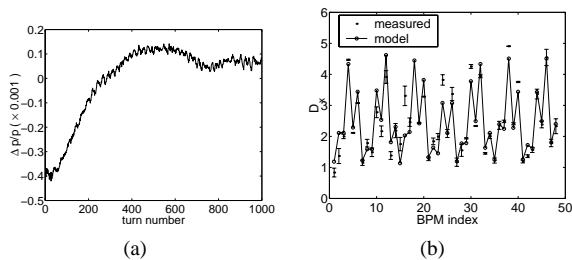


Figure 4: The dispersion mode. (a) the evolution of  $\frac{\Delta p}{p}$ . (b) the measured dispersion function compared to the existing model.

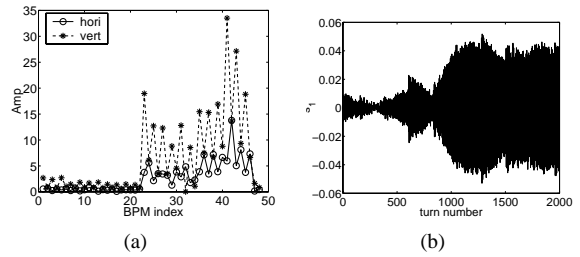


Figure 5: An instability mode in DC data. (a) the amplitude  $A = \sqrt{A_1^2 + A_2^2}$ . (b) the temporal vector.

bility mode is not understood yet.

In AC data, the betatron modes in the cycle allow us to track the betatron tunes throughout the cycle. The linear lattice functions can be measured. Besides the betatron modes, we have also studied synchrotron oscillations during the cycle. More detailed accounts are presented in Ref [4].

### CONCLUSION

We have introduced independent component analysis, an advance signal processing method for synchrotron BPM turn-by-turn data analysis to improve the PCA-based model independent analysis (MIA). This new method has demonstrated its capability in isolating the underlying physical sources in BPM data through simulation studies and the application to Fermilab Booster. By separating the betatron modes we can measure the beta functions and phase advances with better precision. The linearly coupled betatron motions are decomposed to normal modes. It also allows the study of synchrotron motions and other factors that affect the beam transverse motions. This method has the potential to be a powerful diagnostic tool for synchrotrons.

### ACKNOWLEDGEMENTS

We would like to thank the Booster staff and operators for their help in the measurements, W. Guo for the helpful discussions with him.

### REFERENCES

- [1] J. Irwin, C.X. Wang, and Y.T. Yan, PRL **82**, 1684 (1999); Chun-xi Wang, et al. PR-STAB **6**, 104001 (2003).
- [2] A. Belouchrani, K. Abed-Merain, J.F. Cardoso, and E. Moulines, IEEE Trans. Signal Processing, **48**, 900, (2003).
- [3] J. F. Cardoso and A. Souldoumiac, SIAM J. Mat. Anal. Appl., **17**, 161, (1996).
- [4] X. Huang, S.Y. Lee, E. Prebys, R. Tomlin, submitted to PRSTAB (2005).
- [5] W. Guo, private communications.